One influenza virus particle packages eight unique viral RNAs as shown by FISH analysis

Yi-ying Chou[a,1], Reza Vafabakhsh[b,c,1], Sultan Doğanay[d], Qinshan Gao[a], Taekjip Ha[b,c,d], and Peter Palese[a,e,2]

Departments of [a]Microbiology and [e]Medicine, Mount Sinai School of Medicine, New York, NY 10029; and [b]Howard Hughes Medical Institute, [c]Department of Physics, and [d]Center for Biophysics and Computational Biology, University of Illinois at Urbana–Champaign, Urbana, IL 61801

Contributed by Peter Palese, April 10, 2012 (sent for review February 28, 2012)

Influenza A virus possesses a segmented genome of eight negative-sense, single-stranded RNAs. The eight segments have been shown to be represented in approximately equal molar ratios in a virus population; however, the exact copy number of each viral RNA segment per individual virus particles has not been determined. We have established an experimental approach based on multicolor single-molecule fluorescent in situ hybridization (FISH) to study the composition of viral RNAs at single-virus particle resolution. Colocalization analysis showed that a high percentage of virus particles package all eight different segments of viral RNAs. To determine the copy number of each RNA segment within individual virus particles, we measured the photobleaching steps of individual virus particles hybridized with fluorescent probes targeting a specific viral RNA. By comparing the photobleaching profiles of probes against the HA RNA segment for the wild-type influenza A/Puerto Rico/8/34 (PR8) and a recombinant PR8 virus carrying two copies of the HA segment, we concluded that only one copy of HA segment is packaged into a wild type virus particle. Our results showed similar photobleaching behaviors for other RNA segments, suggesting that for the majority of the virus particles, only one copy of each RNA segment is packaged into one virus particle. Together, our results support that the packaging of influenza viral genome is a selective process.

genome packaging | single-molecule imaging | viral ribonucleoprotein complex

Influenza viruses possess a lipid envelope that harbors the glycoproteins hemagglutinin (HA), neuraminidase (NA), and the matrix protein 2 (M2). The core of the virus comprises viral ribonucleoprotein complexes (RNPs) consisting of viral RNAs, nucleoproteins (NP), and three RNA polymerase proteins (PB2, PB1, and PA). The virus genome is composed of eight negative-sense, single-stranded RNA segments: namely PB2, PB1, PA, NP, HA, NA, M, and NS. One of the critical steps in influenza virus infection is the packaging of its segmented genome into the budding virions (1). The segmented genome confers an evolutionary advantage that allows the genes from different virus strains to shuffle and reassort, creating progeny viruses with unique characteristics (2, 3). However, this segmented nature of viral RNA also complicates the process of genome packaging because at least one complete set of eight viral RNA segments has to be packaged into a virus particle to produce infectious progeny. The mechanism by which influenza virus ensures correct packaging of its genome is still unclear.

Two models have been proposed for the incorporation of influenza viral RNAs: (*i*) the random incorporation model (4, 5); and (*ii*) the selective incorporation model (6–13). The random incorporation model proposes that a sufficient number of viral RNAs are randomly chosen to be packaged that will give a reasonable proportion of viable virions that contain at least one copy of each RNA segment (4). The selective incorporation model suggests that a virus particle packages no more than eight viral RNPs and each viral RNA segment contains unique features that allow the viral RNAs to be recognized and distinguished from other segments. The latter being the currently favored hypothesis is supported by: (*i*) EM analyses showing budding virions incorporating eight viral RNPs arranged in a "7+1" architecture (14–17); and (*ii*) segment-specific packaging sequences located at the terminal ends of all eight viral RNAs had been identified by virtue of reverse genetics (6, 8, 10, 11, 18, 19). Even though there has been growing evidence supporting the selective packaging method, conclusive proof that the eight viral RNPs observed in a budding virion are each different is still lacking. Earlier studies using electrophoresis of RNA showed that viral segments were presented at an approximately equal molar ratio within a purified virus preparation (20, 21), but no study has been performed to determine how the incorporated viral segments were segregated into individual virus particles. Recent studies using electron tomography showed the viral RNPs incorporated in the budding virions possess different lengths; however, only a few virus particles were analyzed, and the segments with similar length could not be differentiated by this method (14, 22). The development of single-particle approaches has allowed the characterization of virus particles and events in the virus life cycle that might have been missed in the observations of the entire virus population (23–25). Therefore, to study the genome packaging of influenza viruses, methods that allow stoichiometric analysis of viral RNAs within single-virus particles with individual RNA sensitivity are required.

Herein, we have designed a scheme which allows the detection and quantification of the viral RNAs within influenza virions at single-virus resolution. We applied the single-molecule (sm)FISH technique (26) to surface immobilized virus particles to quantify the packaged viral RNAs. With this approach, we have shown that most if not all influenza virus particles package heterogeneous viral RNAs and each viral RNA segment was packaged only once. These data provide direct evidence that the packaging mechanism in the influenza virus is very robust and the majority of virus particles package the unique eight viral RNAs.

Results

FISH Analysis at Single-Virus Particle Level. We used prism-type total internal reflection fluorescence microscopy (TIRF) (27) to study individual virus particles immobilized on the slide surface. To abolish nonspecific attachment of virus particles, the slide surface was passivated with an inert polymer (PEG) sparsely supplemented with biotinylated polymer. Virus particles were immobilized on the surface through biotinylated antibodies against the influenza hemagglutinin (HA) protein, which were specifically attached to NeutrAvidin molecules bound to biotinylated polymers on the surface (Fig. 1*A*). To quantify the viral RNA composition of virus particles, we performed smFISH on virus particles immobilized on the microscope slides (28). Because viral RNAs

Author contributions: Y.-y.C., R.V., S.D., and P.P. designed research; Y.-y.C., R.V., and S.D. performed research; R.V., Q.G., and T.H. contributed new reagents/analytic tools; Y.-y.C., R.V., and S.D. analyzed data; and Y.-y.C., R.V., T.H., and P.P. wrote the paper.

The authors declare no conflict of interest.

[1]Y.-y.C. and R.V. contributed equally to this work.

[2]To whom correspondence should be addressed. E-mail: peter.palese@mssm.edu.

This article contains supporting information online at www.pnas.org/lookup/suppl/doi:10.1073/pnas.1206069109/-/DCSupplemental.

are packaged within the virus envelope, the immobilized virus particles were fixed with 4% (wt/vol) paraformaldehyde and the viral membrane was then permeabilized with 0.25% Triton-X 100. FISH DNA probes, each labeled with one fluorophore, were used to hybridize to the specific target RNA. We first validated the assay by immobilizing influenza A/Puerto Rico/8/34 (PR8) virus and performing smFISH using a mixture of 48 Cy3-labeled probes against the NA or 48 Cy5-labeled probes against the PB2 RNA segments. In each case, more than 50 fluorescent spots were detected. On the other hand, control experiments using probes against a noninfluenza RNA gene (RIG-I) or blank slides showed very few dim spots (Fig. 1 *B* and *C*). Because the experiments were performed on different channels of the same passivated slide and the concentrations of the antibody, virus particles, and each probe were kept the same, we expected that similar density of virus particles were immobilized on the surface for each experiment. Therefore, the reproducible large contrast in the number of spots (approximately two orders of magnitude) observed between control experiments and experiments probing for influenza viral RNAs demonstrated the high specificity of smFISH in detecting viral RNA segments.

One Influenza Virus Particle Efficiently Copackages Viral RNAs of Different Identities. Having established the platform for FISH analysis at single-virus particle resolution, we determined the copackaging efficiency of two different viral RNA segments into virions by performing hybridization with two probe sets targeting different viral RNAs, one probe set labeled with Cy3 fluorophores and the other labeled with Cy5 fluorophores. Two differently labeled probe sets (Cy3 and Cy5) targeting two different regions of the same viral RNA were used as positive controls and demonstrated the specificity of our technique (Fig. 2*A*). The two sets of probes against different regions of the NA segments showed over 90% (93.1% ± 2.2%) colocalization between Cy3 and Cy5 spots and 84.8% ± 2.0% colocalization for probes against the M

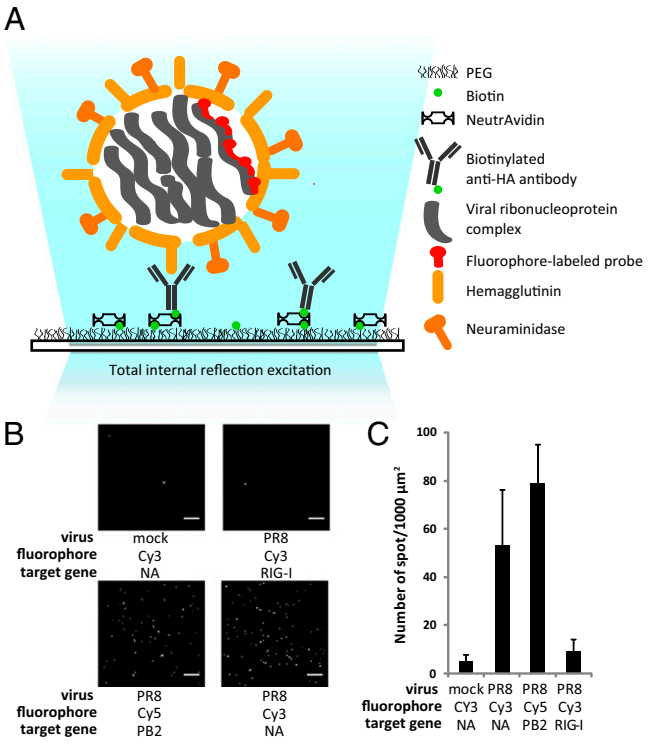

Fig. 1. (*A*) Schematic for FISH analysis on single-virus particle. Viral RNA hybridized with multiple fluorophore-labeled probes is visualized using TIRF microscopy. Biotinylated antibodies against the influenza virus surface protein HA are immobilized on imaging surface passivated with PEG and supplemented with biotinylated PEG and NeutrAvidin. Influenza virus particles are captured onto the imaging surface with the immobilized anti-HA antibodies. FISH is performed on virus particles that are captured, fixed, and permeabilized on the imaging surface. (*B*) TIRF images of FISH signals from hybridization reactions using a mixture of 48 DNA probes singly labeled with fluorophores targeting viral RNA on a blank slide (no immobilized virus), PR8 virus-immobilized slides, and FISH signals from hybridization reactions on PR8 virus-immobilized slide using 48 Cy3-labled probes against the RIG-I mRNA are shown. (*C*) Average number of fluorescent spots per 1,000 μm^2 is shown (number of fields, $n > 10$).

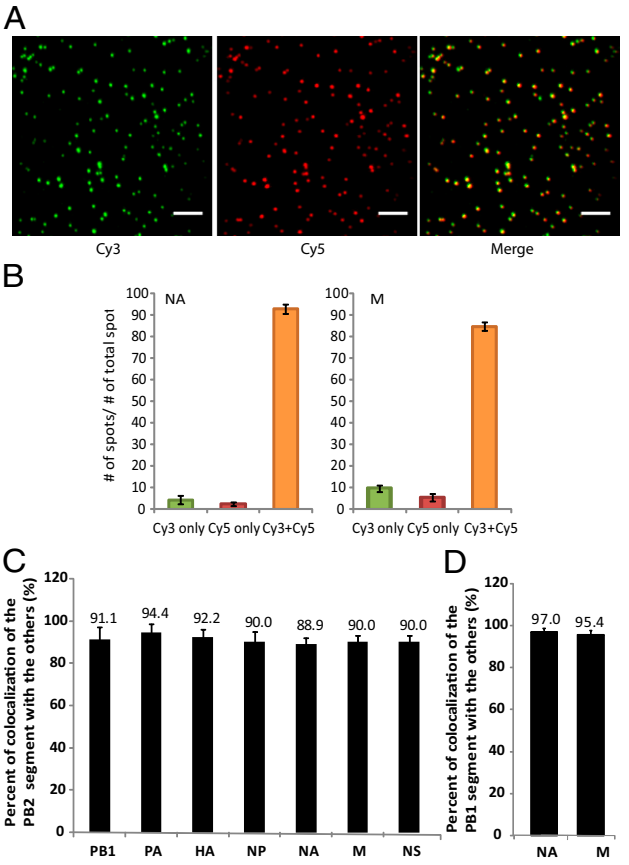

Fig. 2. Copackaging of different viral RNA segments into a virus particle. (*A*) One set of representative TIRF images for colocalization analysis is shown here. Immobilized PR8 virus particles were hybridized with 23 Cy3-labeled probes and 23 Cy5-labeled probes against the viral RNA NA segment. The Cy3 and Cy5 probe sets were targeting distinct regions of the NA segment. TIRF images of particles labeled with Cy3 probes (*Left*) and Cy5 probes (*Center*) are shown. The overlay image of the two images is shown (*Right*). (Scale bar: 5 μm.) (*B*) Colocalization efficiency of two fluorescence probe sets targeting the same viral RNA. FISH analyses were carried out on PR8 virus immobilized imaging surfaces using 23 Cy3-labeled probes and 23 Cy5-labeled probes against the NA viral segments or 16 Cy3-labeled probes and 16 Cy5-labeled probes against the M viral segments. The percentages of the number of the Cy3-only spots, the Cy5-only spots and the dual-labeled spots over the total number of spots are plotted. (*C*) Colocalization efficiency of the PB2 segment with the PB1, PA, HA, NP, NA, M, and NS segment is shown. For each pair with the PB2 segment tested, 48 Cy3-labeled probes targeting the PB2 segment were mixed with 15 Cy5-labeled probes targeting the paired segment. (*D*) Colocalization efficiency of the PB1 segment with the NA and M segment. FISH analysis was performed by mixing 48 Cy3-labeled probes targeting the PB1 segment with 15 Cy5-labeled probes targeting either the NA or M segments. The colocalization efficiency is calculated as the number of Cy3 and Cy5 colocalized spots over the total number of Cy3 spots. The data shown are normalized by setting the colocalization efficiency of Cy3 and Cy5 probe sets against the NA segment as 100% (see *B*). Error bars denotes SD ($n > 10$).

segment. The percentages of spots showing only Cy3 or Cy5 signals were comparable and were all below 10% in both cases, indicating that the two differently labeled probe sets share similar sensitivity and detect comparable number of viral RNAs (Fig. 2*B*). Although we observed similar intensity distributions between colocalized spots and spots that did not colocalized, intrinsic defects of some viral RNAs or the limitation of our detection and analysis would explain why we did not see 100% colocalization between the Cy3 and Cy5 fluorescence spots. To determine whether influenza virus efficiently packages viral RNA of different identities, we first tested the copackaging efficiency of the Cy3 probe-labeled PB2 segment paired with the other seven viral RNA segments that were labeled with Cy5 probes. Colocalization efficiency was calculated as the number of colocalized spots over the number of Cy3 fluorescent spots corresponding to the PB2 segment. The PB2 segment showed high percentages of colocalization with all of the other viral RNA tested (Fig. 2*C*). These results demonstrated that the PB2 segment was efficiently copackaged with other viral RNAs into virus particles and that over 50% of virus particles that package the PB2 segments also package the other seven segments. This percentage comes from multiplying the colocalization efficiencies of viral segments paired with the PB2 segment ($0.911 \times 0.944 \times 0.922 \times 0.9 \times 0.889 \times 0.9 \times 0.9$). In all these experiments, the Cy3 probes against the PB2 segment and the Cy5 probes targeting the paired viral RNAs detected a comparable number of spots. This effectively showed that the other seven segments efficiently copackaged with the PB2 segment as well (Fig. S1). Colocalization analysis of the PB1 segment with the NA segment and the M segment also showed percentages of colocalization over 90% (97.0% ± 1.86% for PB1 and NA, 95.4% ± 2.93% for PB1 and M) (Fig. 2*D*). These data show that influenza virus proficiently packages heterogeneous viral RNAs into virons.

One Copy of Each Viral RNA Segment Is Packaged into a Virus Particle. To understand whether the heterogeneous viral RNAs packaged into the virus particles were unique, we determined the copy number of each viral RNA segment being packaged. If a viral RNA segment is unique in the virus particle, then only one copy of that RNA would be detected by the single-virus particle FISH analysis. The number of viral RNAs being packaged can be determined by counting the number of hybridized probes in a fluorescent spot by photobleaching analysis.

We first performed single-virus particle FISH and photobleaching analysis on the HA viral RNA segment in the PR8 virus. In this experiment, 15 HA-targeting probes singly labeled with Cy5 were mixed for hybridization. Movies of several imaging areas were obtained, and the time traces of fluorescence intensity for the spots were analyzed. As the fluorophore on each probe photobleaches over time, the fluorescence intensity diminishes over time, yielding a step-wise profile. The number of steps corresponds to the number of probes that are hybridized to the HA target (Fig. 3*A*). Because 15 probes were used for hybridization and the binding efficiencies of the probes were different, the number of probes bound to a single viral RNA would not be identical. To address this question, we counted the number of photobleaching steps for over 800 fluorescent spots corresponding to the HA viral RNA. Fig. 3*D* shows the distribution of the number of photobleaching steps for FISH probes against the HA viral RNA in the PR8 virus particles. A single peak around seven steps was observed, demonstrating that, on average, seven probes are likely to hybridize with an HA viral segment in a single-virus particle using our experimental design.

To demonstrate that PR8 virus particles package only one copy of the HA segment instead of two or more copies, we used reverse genetic techniques to generate a virus that carries two copies of the HA gene. It has been shown previously that influenza viral RNAs possess segment specific packaging sequences governing the incorporation of viral RNAs into the virions. A recombinant virus

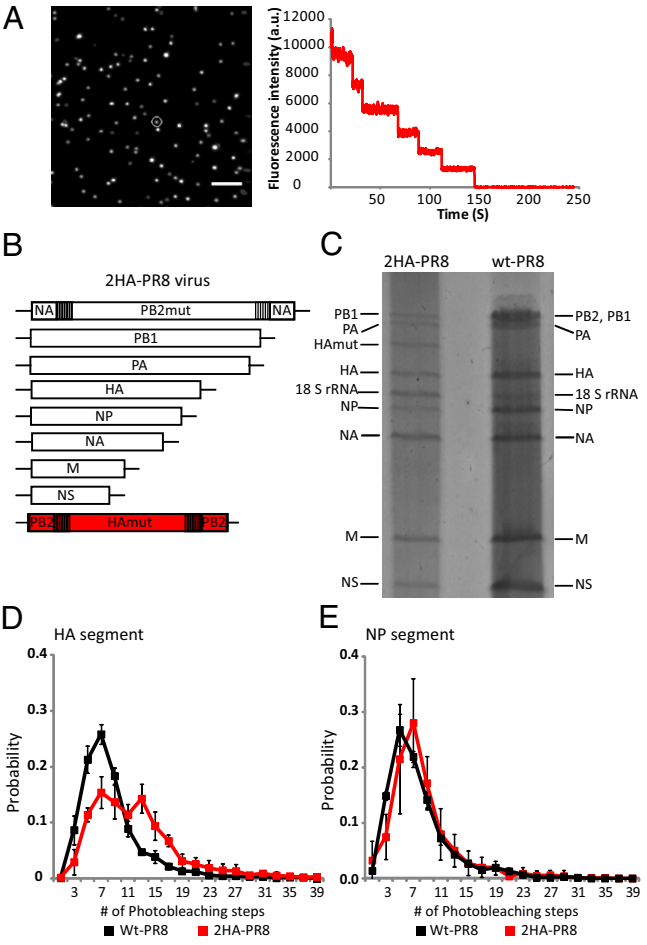

Fig. 3. PR8 virus particle packages one copy of the HA segment. (*A*) Photobleaching analysis of the HA viral RNA in PR8 viruses hybridized with 15 Cy5-labeled probes. *Right*, An average of 30,000 TIRF movie frames of a short movie taken at an imaging area which was consistently excited for 5 min. The graph represents a typical plot of total fluorescence intensity versus time for a Cy5 spot exhibiting a seven-step photobleaching behavior. This plot corresponds to the circled spots in the averaged TIRF image (*Left*). (*B*) Genome structure of the 2HA-PR8 virus. Seven A/Puerto Rico/8/34 ambisense plasmids (pDZ-PB1, pDZ-PA, pDZ-HA, pDZ-NP, pDZ-NA, pDZ-M, pDZ-NS) and two chimeric constructs, pDZ-NA-PB2mut-NA and pDZ-PB2-HAmut-PB2 (*Material and Methods*) were used to generate the 2HA-PR8 virus by reverse genetics. (*C*) Analysis of viral RNA packaging in 2HA-PR8 virus. Purified viral RNAs from the 2HA-PR8 virus and PR8 virus were resolved using a 2.8% acrylamide gel, followed by silver staining. The identities of the bands were labeled based on their sizes and previous findings. (*D*) Histogram of the photobleaching steps analyzed for the FISH probes hybridized HA segment in PR8 and 2HA-PR8 viruses. Error bars denote SDs ($n \geq 5$). (*E*) Histogram of the photobleaching steps analyzed for the FISH probes hybridized NP viral RNA in PR8 virus and 2HA-PR8 virus. The black squares and solid black lines represent the PR8 virus, and the red squares and solid red lines represent the 2HA-PR8 virus. Error bars denote SDs ($n \geq 3$).

carrying one additional segment had been successfully generated by engineering the segment-specific packaging sequences in the viral genome (29). Applying the same principle, we exchanged the packaging signals for the PB2 segment with the NA segment-specific packaging signals and the packaging sequences that remained within the PB2 ORF were inactivated with serial synonymous mutations (NA-PB2mut-NA segment). The PB2 packaging signals were then used to flank the additional HA ORF, which also contained serial silent mutations at both terminals to inactivate the residual packaging sequences (PB2-HAmut-PB2 segment) (Fig. 3*B*). The 2HA-PR8 virus carries the mutated PB2 segment and

two HA segments. To determine whether both HA segments were incorporated into the virus particles, viral RNA extracted from purified 2HA-PR8 virus was resolved using RNA electrophoresis, followed by silver staining. The PB2-HAmut-PB2 segment migrating between the PA segment and the HA segment was observed, showing that the additional HA segment was incorporated into virus particles. The intensity of the band was similar between wild-type HA segment and the PB2-HAmut-PB2 segment, suggesting that both segments were incorporated into virus particles at comparable efficiency (Fig. 3*C*). It is of note that the NA-PB2mut-NA segment was not resolved by RNA electrophoresis demonstrating that a low number of virus particles package this segment. Taken together, these data suggest that a virus population incorporated two segments containing the HA ORF existed in the 2HA-PR8 virus.

To test whether the photobleaching analysis is able to resolve the number of target segments packaged into virus particles, we performed FISH and photobleaching analysis on 2HA-PR8 virus under the same experimental conditions as the wild type. The histogram of photobleaching steps for the HA segment in the 2HA-PR8 virus showed an increased breadth of the overall curve than for the HA segment in the wild-type PR8 virus, indicating that the photobleaching analysis was able to detect differences in the number of target segments packaged into virus particles. Two peaks were observed in the histogram of the HA segment in 2HA-PR8 virus. The first peak occurred around seven steps, which was the same peak step number as for the PR8 virus. The second peak appeared around 13 steps, which is approximately double the step number of the first peak. These results showed that in the 2HA-PR8 virus population, there were some virions containing the same number of HA segment as the wild-type PR8 virus and some virus particles that packaged as twice as many. To further confirm that the 2HA-PR8 virus did not exhibit intrinsic disorganization of viral RNA packaging, we performed FISH and photobleaching analysis using 15 Cy5 probes against the NP segment in the wild-type PR8 and 2HA-PR8 virus. The photobleaching step histograms of NP segment in both viruses displayed single-peak distributions, demonstrating that 2HA-PR8 virus was not defective in packaging unmodified viral RNAs and the stoichiometry of the packaged NP segment was the same as that of the wild-type virus (Fig. 3*E*). Because it was unlikely that a 2HA-PR8 virus packaged four copies or more HA segments, these data strongly suggested that the double-peak distribution seen was representative of two viral HA segments being incorporated into a single virion. Therefore, the single peak distribution of the photobleaching step histogram seen for the HA segment in PR8 virus arguably represents only one copy of the HA segment packaged into virus particles. Our data also strongly suggests that a single copy of NP is incorporated into a single virion.

We next wanted to assess whether only a single copy of the other viral RNA segments was package into PR8 virus particles. We performed FISH and photobleaching step analysis for the other six segments: PB2, PB1, PA, NA, M, and NS. For each viral segment analyzed, 15 Cy5 probes were mixed for the hybridization reaction, and bleaching steps for more than 500 fluorescence spots were counted. The histograms of the photobleaching steps for the segments examined all exhibited single-peak profiles (Fig. 4). Gaussian distribution fits to the photobleaching histograms in Fig. 4 showed that more than 90% of the virus particles package a single copy of a specific gene (Fig. S2). It is of note that the remaining 10% of the spots, which exhibit high number of photobleaching steps, likely represents self aggregation of the virus particle (10–20%) (30) and virus particles immobilized within diffraction limited area. Therefore, the majority of the virus particles contain a single copy of a specific gene. Because a high proportion of influenza virus particles package eight different viral RNA segments (Fig. 2) and each segment was packaged with the same copy number, these results provided strong evidence

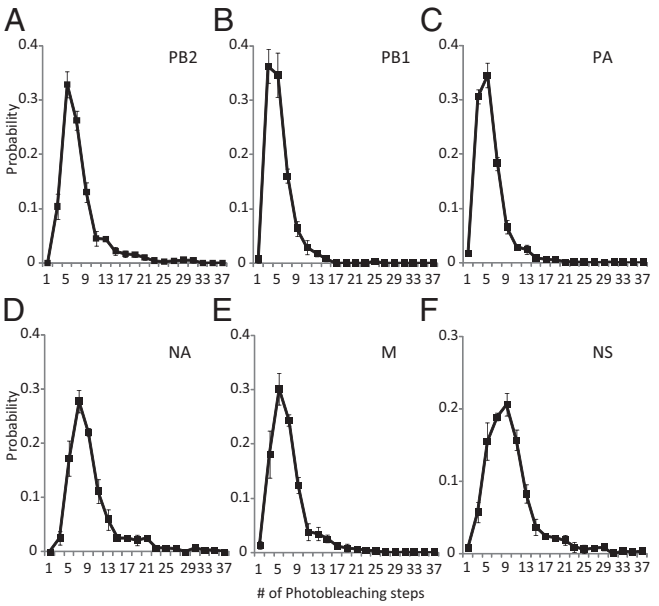

Fig. 4. PR8 virus packages single copy of each viral RNA segment. Histograms of the photobleaching analysis are shown for the PB2 (*A*), PB1 (*B*), PA(*C*), NA (*D*), M (*E*), and NS (*F*) segments in the PR8 virus. Error bars denote SDs. $n \geq 3$.

that the majority of influenza virus particles contain one copy of each viral segment.

In conclusion, we have demonstrated with the two-color FISH and photobleaching-step analysis on individual virus particles that a large proportion of virus particles packaged heterogeneous viral RNPs and a single copy of each gene was packaged into a virion in most cases. Therefore, we have provided evidence that an influenza virus particle packages eight unique viral RNAs and that this selective packaging process is efficient.

Discussion

In this study, we have established an experimental system assay based on smFISH to study the packaged RNA compositions in individual virus particles. Our results demonstrate that eight unique viral RNAs are packaged within a single influenza virion. This technique created a powerful tool to understand the stoichiometry of viral RNAs inside virus particles and provided quantitative data on the subpopulations of different viruses.

In this report, two-color FISH analysis on virus particles provided direct measurements of the probability of two different viral RNA segments being copackaged into the same virion. The PB2 segment was shown to be copackaged with each of the other viral RNA segments at efficiencies around 90%. This indicated that a large proportion of virions that package the PB2 segment also package the other seven segments. It is of note, however, that colocalization between Cy3 and Cy5 in our control experiments was only ~90% (Fig. 2*B*). Because we would expect the controls to have 100% colocalization, it is possible that we are underestimating the percentage of virions that incorporate all eight segments. Nevertheless, these results quantitatively showed that heterogeneous viral RNA segments are selectively packaged within an influenza virion with high efficiency.

The precise mechanisms and viral elements essential for the selection process are largely unknown. Segment-specific packaging sequences have been discovered for all eight viral RNA segments by virtue of reverse genetics and mutation analysis (6–9, 11, 18, 19). Several studies have shown that mutations introduced into the packaging signals of one segment of a viable virus affects the incorporation of that segment into virions, as well as the incorporation of other segments to different degrees (6, 8, 18). For

example, synonymous mutations introduced into the HA-packaging sequences reduced the incorporation of not only the HA segment but also of the PB2 segment, as shown by quantitative PCR of viral RNAs extracted from viruses (8). These studies have demonstrated that there are interactions among different viral RNA segments that could affect their incorporations into virus particles; however, there have not yet been studies to assess the role that packaging signals, or general interactions among viral genes, play in the copackaging of different viral RNA segments. With the technology reported here, we were able to quantify the numbers of virus particles containing two different viral RNA segments, allowing for the calculation of the probability of these two segments being copackaged. This experimental setup provided a measurable parameter for influenza virus and can be further applied to study the effect of identified packaging signals on the copackaging efficiency of viral RNAs or the discovery of viral elements governing the selective packaging process.

The selection process of influenza viral RNA packaging was controlled not only for the identities of the segments packaged but also for their copy number. We have applied photobleaching analysis to resolve the copy number of a specific viral RNA segment that is packaged into one virion. Results from the analysis of the HA segment in wild-type PR8 and 2HA-PR8 viruses showed that only one copy of the HA segment was incorporated per PR8 virus particle. Analysis of other viral RNA segments also suggested that eight single copies of each viral RNA segment was packaged into one virus particle. These data, together with earlier studies showing that the eight segments exhibited approximately equal molar ratio in RNA extracted from purified viruses (21), strongly suggest that each of the eight viral RNA segments are equally distributed into individual virus particles. Given that EM analyses have shown budding influenza virions with eight viral RNPs (14, 15, 22) and the data presented here showing high copackaging efficiency of heterogeneous viral RNA segments (Fig. 2), we believe that in a large proportion of the virus population, one copy of each of the eight viral RNA segments is indeed packaged into one influenza virus particle.

In conclusion, we have established an experimental system for single-molecule sensitivity FISH analysis on individual virus particles. This technique allowed us to understand the stoichiometry and composition of the segmented viral RNAs in influenza virus particles. We have shown with this technique that one influenza virus particle packages eight unique viral RNA segments, providing quantitative evidence that the genome packaging of influenza virus is a highly selective process. This strategy can be further applied to study the packaging mechanisms of other viruses with a segmented genome.

Materials and Methods

Cell and Viruses. The 293T cells were obtained from the American Type Culture Collection and were maintained in DMEM supplemented with 10% FCS. The PR8 virus and the recombinant 2HA-PR8 virus were grown in 10-d-old specific-pathogen-free chicken embryos (Charles River Laboratories, SPAFAS).

Plasmid construction. (*i*) Generation of PB2-HAmut-PB2 construct. The GFP ORF from a previously made PB2-GFP-PB2 construct (29) was replaced with the PR8 virus HA ORF carrying serial silent mutations on the two ends [designated as HAmut (31)], generating the PB2-HAmut-PB2 construct. NheI and XhoI restriction sites were used for cloning. (*ii*) The NA-PB2mut-NA construct was described previously (29).

Reverse Genetics for the 2-HA PR8 Virus. Generating recombinant 2-HA PR8 virus was performed using previously described methods (29).

Virus Purification. Wild-type PR8 virus and the 2-HA PR8 virus were grown in 10-d embryonated chicken eggs (Charles River Laboratories, SPAFAS) at 37 °C for 48 and 60 h, respectively. The embryos were then killed, and the allantoic fluid was harvested. The allantoic fluid was clarified by centrifugation at 3,000 × g at 4 °C for 30 min. The clarified allantoic fluid was then layered on a 20% sucrose cushion and centrifuged at 4 °C, 25,000 rpm for 2 h using a Beckman rotor SW28. The pelleted virus was resuspended in 1XNTE buffer [100 mM NaCl, 10 mM Tris-HCl (pH 7.4), 1 mM EDTA] and layered onto a 10–30% iodixanol density gradient (Sigma-Aldrich) for centrifugation at 25,000 rpm for 3 h at 4 °C. The virus was extracted from the gradient using a syringe and pelleted by centrifugation at 4 °C, 25,000 rpm for 1.5 h. The purified virus was resuspended in 1XNTE and stored at −80 °C before use.

Polyacrylamide Agarose Gel Electrophoresis for Purified Viral RNA. The viral RNA for gel electrophoresis was extracted from purified viruses using TRIzol reagent (Invitrogen) following methods that have been described previously (32).

Single-Virus Particle Immobilization and FISH. Virus particle immobilization and single-molecule imaging were performed as described previously (28) with several modifications. In brief, flow chambers were prepared on polyethylene glycol (PEG) passivated slides supplemented with biotinylated PEG and coated with NeutrAvidin (Thermo). To capture influenza virus particles, biotinylated mouse monoclonal anti-hemagglutinin antibodies were immobilized by incubating the antibody at a 15 nM concentration on the chambers for 20 min at room temperature. The virus was diluted in T50 buffer [10 mM Tris-HCl (pH 8.0), 1 mM EDTA, 50 mM NaCl] and incubated for 30 min at room temperature over the surface with immobilized antibody. The PR8 virus was diluted 1:150 and the 2-HA PR8 virus was diluted 1:30 from the stock to obtain well-isolated spots on the surface (~250 particles in 2,500-μm^2 imaging area). The unbound antibodies and virus particles were washed away with T50 buffer. The antibodies and virus were then fixed with 4% paraformaldehyde in T50 buffer for 10 min. After one wash with T50 buffer, the virus particles were permeabilized by 10-min incubation with 0.25% Triton X-100 to expose the viral RNPs. The flow chambers were then washed twice with T50 supplemented with 2 mM RNase inhibitor vanadyl ribonucleoside complexes (VRC) (New England BioLabs) before hybridization.

FISH was performed following protocols published previously (26, 33). For each influenza viral RNA, 30–48 probes were designed and synthesized (Biosearch Technologies). The probes were labeled with Cy3 or Cy5 fluorophores and HPLC-purified according to a published protocol (34). The hybridization reactions were carried out by incubating the permeabilized virus with the hybridization solution containing each probe at a 4 nM concentration at 37 °C for 3 h. Different numbers of probes were mixed for the hybridization reactions according to experimental purposes. After hybridization, the virus immobilized surfaces were washed with wash buffer (2× SSC, 10% formamide, and 2 mM VRC) at 37 °C for 30 min and then incubated in 2× SSC before imaging. Single-molecule imaging was performed using a prism-type TIRF microscope, and the single-molecule analysis was performed as described previously (27, 28).

Photobleaching Step Analysis. The single-molecule fluorescence time traces of the hybridized viral RNAs were scored for the number of photobleaching steps by a semiautomated algorithm. Because clean bleaching steps could be identified, the average step size of a single bleaching step was calculated and the total number of photobleaching steps was determined based on the starting fluorescence intensity. All of the fluorescence traces were examined manually; traces with no clean bleaching steps or derived from fluorescent spots exhibiting oval shape (virus particles aggregates) were discarded. For each sample, at least 300 particles were scored.

Colocalization Analysis. Colocalization between Cy3 and Cy5 spots was analyzed similarly as described previously (28, 35). The colocalization efficiency was calculated as the overlap percentage of the number of colocalized spots over the total number of Cy3 spots.

ACKNOWLEDGMENTS. We thank Ming-Ming Zhou and Guillermo Gerona-Navarro for technical assistance in HPLC purification of probes and Natalie Pica for review of the manuscript. This work was supported by Center for Research on Influenza Pathogenesis (CRIP) Grant HHSN266200700010C (to P.P.), National Science Foundation Grants 0646550 and 0822613 (to T.H.), and National Institutes of Health Grant U19AI083025 (to T.H). T.H. is an investigator with the Howard Hughes Medical Institute.

1. Palese P, Shaw ML (2007) Orthomyxoviridae: The viruses and their replication. *Field's Virology*, eds Knipe DM, Howley PM (Lippincott Williams & Wilkins, Philadelphia), Vol 2, pp 1648–1689.
2. Desselberger U, et al. (1978) Biochemical evidence that "new" influenza virus strains in nature may arise by recombination (reassortment). *Proc Natl Acad Sci USA* 75: 3341–3345.
3. Young JF, Palese P (1979) Evolution of human influenza A viruses in nature: Recombination contributes to genetic variation of H1N1 strains. *Proc Natl Acad Sci USA* 76:6547–6551.
4. Enami M, Sharma G, Benham C, Palese P (1991) An influenza virus containing nine different RNA segments. *Virology* 185:291–298.
5. Bancroft CT, Parslow TG (2002) Evidence for segment-nonspecific packaging of the influenza a virus genome. *J Virol* 76:7133–7139.
6. Marsh GA, Rabadán R, Levine AJ, Palese P (2008) Highly conserved regions of influenza a virus polymerase gene segments are critical for efficient viral RNA packaging. *J Virol* 82:2295–2304.
7. Liang Y, Huang T, Ly H, Parslow TG, Liang Y (2008) Mutational analyses of packaging signals in influenza virus PA, PB1, and PB2 genomic RNA segments. *J Virol* 82:229–236.
8. Marsh GA, Hatami R, Palese P (2007) Specific residues of the influenza A virus hemagglutinin viral RNA are important for efficient packaging into budding virions. *J Virol* 81:9727–9736.
9. Muramoto Y, et al. (2006) Hierarchy among viral RNA (vRNA) segments in their role in vRNA incorporation into influenza A virions. *J Virol* 80:2318–2325.
10. Fujii K, et al. (2005) Importance of both the coding and the segment-specific noncoding regions of the influenza A virus NS segment for its efficient incorporation into virions. *J Virol* 79:3766–3774.
11. Fujii Y, Goto H, Watanabe T, Yoshida T, Kawaoka Y (2003) Selective incorporation of influenza virus RNA segments into virions. *Proc Natl Acad Sci USA* 100:2002–2007.
12. Odagiri T, Tashiro M (1997) Segment-specific noncoding sequences of the influenza virus genome RNA are involved in the specific competition between defective interfering RNA and its progenitor RNA segment at the virion assembly step. *J Virol* 71: 2138–2145.
13. Duhaut SD, McCauley JW (1996) Defective RNAs inhibit the assembly of influenza virus genome segments in a segment-specific manner. *Virology* 216:326–337.
14. Fournier E, et al. (2012) A supramolecular assembly formed by influenza A virus genomic RNA segments. *Nucleic Acids Res* 40:2197–2209.
15. Noda T, et al. (2006) Architecture of ribonucleoprotein complexes in influenza A virus particles. *Nature* 439:490–492.
16. Yamaguchi M, Danev R, Nishiyama K, Sugawara K, Nagayama K (2008) Zernike phase contrast electron microscopy of ice-embedded influenza A virus. *J Struct Biol* 162: 271–276.
17. Harris A, et al. (2006) Influenza virus pleiomorphy characterized by cryoelectron tomography. *Proc Natl Acad Sci USA* 103:19123–19127.
18. Hutchinson EC, Curran MD, Read EK, Gog JR, Digard P (2008) Mutational analysis of cis-acting RNA signals in segment 7 of influenza A virus. *J Virol* 82:11869–11879.
19. Liang Y, Hong Y, Parslow TG (2005) cis-Acting packaging signals in the influenza virus PB1, PB2, and PA genomic RNA segments. *J Virol* 79:10348–10355.
20. Hatada E, Hasegawa M, Mukaigawa J, Shimizu K, Fukuda R (1989) Control of influenza virus gene expression: Quantitative analysis of each viral RNA species in infected cells. *J Biochem* 105:537–546.
21. McGeoch D, Fellner P, Newton C (1976) Influenza virus genome consists of eight distinct RNA species. *Proc Natl Acad Sci USA* 73:3045–3049.
22. Noda T, et al. (2012) Three-dimensional analysis of ribonucleoprotein complexes in influenza A virus. *Nat Commun* 3:639.
23. Floyd DL, Harrison SC, van Oijen AM (2009) Method for measurement of viral fusion kinetics at the single particle level. *J Vis Exp* 31:1484.
24. Floyd DL, Ragains JR, Skehel JJ, Harrison SC, van Oijen AM (2008) Single-particle kinetics of influenza virus membrane fusion. *Proc Natl Acad Sci USA* 105:15382–15387.
25. Dilley KA, et al. (2011) Determining the frequency and mechanisms of HIV-1 and HIV-2 RNA copackaging by single-virion analysis. *J Virol* 85:10499–10508.
26. Raj A, van den Bogaard P, Rifkin SA, van Oudenaarden A, Tyagi S (2008) Imaging individual mRNA molecules using multiple singly labeled probes. *Nat Methods* 5: 877–879.
27. Roy R, Hohng S, Ha T (2008) A practical guide to single-molecule FRET. *Nat Methods* 5: 507–516.
28. Jain A, et al. (2011) Probing cellular protein complexes using single-molecule pull-down. *Nature* 473:484–488.
29. Gao Q, Lowen AC, Wang TT, Palese P (2010) A nine-segment influenza a virus carrying subtype H1 and H3 hemagglutinins. *J Virol* 84:8062–8071.
30. Wei Z, et al. (2007) Biophysical characterization of influenza virus subpopulations using field flow fractionation and multiangle light scattering: Correlation of particle counts, size distribution and infectivity. *J Virol Methods* 144:122–132.
31. Gao Q, Palese P (2009) Rewiring the RNAs of influenza virus to prevent reassortment. *Proc Natl Acad Sci USA* 106:15891–15896.
32. Gao Q, Brydon EW, Palese P (2008) A seven-segmented influenza A virus expressing the influenza C virus glycoprotein HEF. *J Virol* 82:6419–6426.
33. Femino AM, Fay FS, Fogarty K, Singer RH (1998) Visualization of single RNA transcripts in situ. *Science* 280:585–590.
34. Raj A, Tyagi S (2010) Detection of individual endogenous RNA transcripts in situ using multiple singly labeled probes. *Methods Enzymol* 472:365–386.
35. Ulbrich MH, Isacoff EY (2007) Subunit counting in membrane-bound proteins. *Nat Methods* 4:319–321.